chapter 6

Cooling of cooked ready-to-eat meats and computer simulation

Lihan Huang and Shiowshuh Sheen

Contents

6.1 Introduction

Clostridium perfringens is a spore-forming foodborne human pathogen that frequently complicates the safety of ready-to-eat (RTE) meat and poultry products. This microorganism is ubiquitously distributed in the environment, including soil, water, air, and intestinal tracts of many warm-blooded animals and humans (Brynestad and Granum, 2002; Juneja et al., 2001). As a spore former, this organism can survive relatively harsh environmental conditions and enter raw foods in the form of spores. As a result, raw materials used in preparing RTE meat and poultry products may be natural carriers of *C. perfringens* spores.

C. perfringens is a typical Gram-positive, anaerobic bacterium that thrives particularly well under conditions where oxygen is absent or the level is low. Cooking of meat and poultry products may create a condition that allows this microorganism to grow and multiply. Under normal cooking conditions, a thermal treatment process is usually designed to induce certain physical and chemical changes in RTE meats. Vegetative cells of common foodborne pathogens, such as *Listeria monocytogenes, Salmonella* spp., and *Escherichia coli* O157:H7, along with other spoilage microorganisms, are generally eliminated in the cooking step. However, the temperature conditions used in the cooking step are often insufficient to kill spores of *C. perfringens*. Instead, the spores may be activated during cooking. Since cooking expels oxygen from the food and eliminates background flora, the spores may germinate, outgrow, and multiply during cooling.

Under anaerobic conditions, germinated *C. perfringens* can grow rapidly at temperatures between 30°C and 47°C, a range of temperature that spores are exposed to during cooling (Craven, 1980). According to the literature, the optimum growth temperature for this microorganism is between 43°C and 47°C (Hall and Angelotti, 1965).

Cooling of cooked products is a critical step to prevent the germination, outgrowth, and multiplication of *C. perfringens* in cooked meats. As cooked products are cooled from their final cooking temperature to their final storage temperature, they are exposed to temperatures between 50°C and 10°C, a range suitable for the growth of this organism. At the optimum temperatures, the generation time can be as short as 7.1 min in cooked ground beef (Willardsen et al., 1979). Due to the high growth rate of *C. perfringens* at optimum temperatures, rapid cooling is essential to prevent outbreaks caused by cooked meats. Because of the importance of cooling in preventing the growth of *C. perfringens*, the U.S. Department of Agriculture (USDA) Food Safety and Inspection Service (FSIS) has issued

guidelines that require the internal temperature of cooked meats during a cooling process be reduced from 54.4°C (130°F) to 26.7°C (80°F) in less than 1.5 h, and from 26.7°C to 4.4°C (40°F) in less than 5 h. If a meat processor cannot meet this "safe harbor," it is necessary to show that the custom cooling regimen (or in the case of a process deviation) would result in less than a 1-log increase in *C. perfringens* and no growth of *Clostridium botulinum*. In the event of process deviation, mathematical growth models can be used to assess the extent of *C. perfringens* growth and evaluate the safety of the implicated meat product. To estimate the potential growth of Clostridia in cooked or partially cooked meat products, it is necessary to understand the growth kinetics of microorganisms and develop mathematical models that accurately describe the microbial growth behaviors.

6.2 *Models and methods for microbial growth under isothermal conditions*

The growth of bacteria in foods usually follows a sigmoidal trend and is affected by both intrinsic and extrinsic conditions. Examples of extrinsic conditions include temperature and time, which defines the temperature history of a food. Intrinsic conditions are the physical and chemical properties of a food, which may include pH, salt level, and the existence and concentration of antimicrobial agents. Under normal conditions, bacterial growth typically exhibits three sequentially progressing phases. The first phase is the lag phase, during which no apparent change in the counts of bacteria can be observed. The second phase is the exponential phase, during which the number of bacteria increases exponentially. The last phase is the stationary phase, in which the number of bacteria reaches the maximum. The duration of the lag phase (λ) and the bacterial growth rate (K) in the exponential phase are affected primarily by temperature, but they also are influenced by many intrinsic conditions.

To estimate bacterial growth, a model must be able to describe these three distinct phases. A primary model is a mathematical model capable of describing the three-phase time-dependent growth curve under constant temperature conditions. Since λ and K are affected by temperature, a secondary model is developed to describe the effect of temperature on these two parameters. A tertiary model is a mathematical model that correlates kinetic parameters (λ and K) to both intrinsic and extrinsic factors, such as temperature, pH, salt concentration, water activity, and other relevant ingredients. The combined application of the models of different levels makes it possible to estimate the growth of microorganisms under static or dynamic conditions.

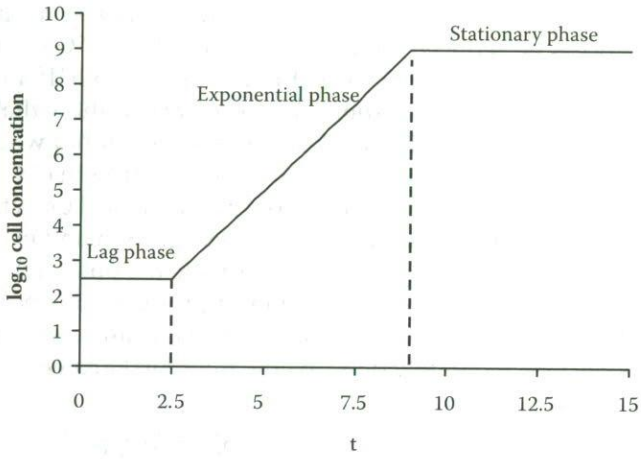

Figure 6.1 A hypothetical isothermal growth curve with three distinctive growth phases (initial cell concentration = 2.5 logs, lag phase = 2.5, specific growth rate = 1.0 log per unit time, final cell concentration = 9.0 logs).

6.2.1 *Primary models*

The primary models are the basic block for predictive microbiology. Models at the primary level are designed to describe the growth of the microorganism as a function of time under isothermal conditions. Figure 6.1 illustrates a hypothetical growth curve with the three-phase growth phenomenon of microorganisms under isothermal conditions. A primary model must be a smooth curve that gradually progresses from the lag phase, through the exponential phase, and to the final stationary phase.

6.2.1.1 *Empirical models*

Primary models of different complexity have been developed and used in estimating the microbial growth. The simplest models are empirical models such as those modified from the original Gompertz and logistic equations. Both modified Gompertz and logistic models use a transition function that allows the curves to gradually progress from the lag phase to the stationary phase. For both modified Gompertz and logistic models, the general mathematical equation is expressed as

$$L(t) = L_{max} + (L_{max} - L_0)S(t) \qquad \text{Eq. 6.1}$$

In Eq. 6.1, $L(t)$ is the logarithm (base 10) of the counts of microorganisms at any given time t; L_{max} is the logarithm of the maximum counts of microorganisms; L_0 is the logarithm of the initial counts; and $S(t)$ is the sigmoidal function, which is written as

$$S(t)=\begin{cases}\exp\left\{-\exp\left[-\mu\left(t-M\right)\right]\right\} & \textit{Gompertz}\\ \dfrac{1}{1+\exp\left[-\mu\left(t-M\right)\right]} & \textit{Logistic}\end{cases} \qquad \text{Eq. 6.2}$$

In Eq. 6.2, M is the inflection point of a growth curve, and μ is the relative rate constant at $t = M$, which is the point of the curve where the maximum slope is located. From Eqs. 6.1 and 6.2, two of the most important growth parameters can be derived. The first parameter is the duration of a lag phase (λ) under an isothermal condition, which can be calculated from

$$\lambda=\begin{cases}M-\dfrac{1}{\mu} & \textit{Gompertz}\\ M-\dfrac{2}{\mu} & \textit{Logistics}\end{cases} \qquad \text{Eq. 6.3}$$

The other parameter is the specific or exponential growth rate, K, which is located at the point where $t = M$, and can be calculated from

$$K=\begin{cases}\dfrac{L_{max}-L_0}{e}\mu & \textit{Gompertz}\\ \dfrac{L_{max}-L_0}{4}\mu & \textit{Logistic}\end{cases} \qquad \text{Eq. 6.4}$$

Although slightly different in mathematical characteristics, both modified Gompertz and logistic models can adequately describe microbial growth under isothermal conditions. Figure 6.2 illustrates the comparison between the modified Gompertz and logistic models used to fit the same hypothetical growth curve shown in Figure 6.1. Table 6.1 lists the growth parameters estimated using these two models. It is evident that the specific growth rates and the lag phases are slightly overestimated by the modified Gompertz and logistics models. The major difference between the modified Gompertz model and the modified logistic model

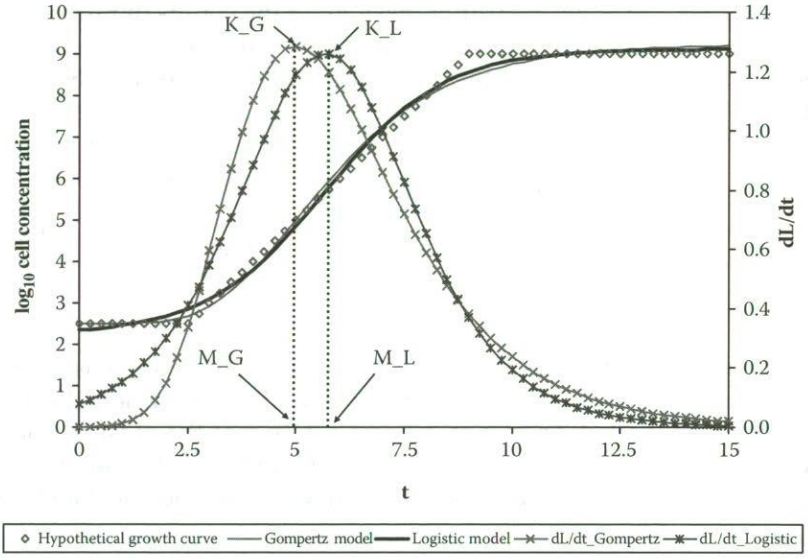

Figure 6.2 Comparison between Gompertz and logistic models used to fit the hypothetical growth curve shown in Figure 6.1.

Table 6.1 Growth Parameters Calculated from the Modified Gompertz and Logistic Models Used to Fit the Growth Curve Shown in Figure 6.1

Parameters	Target Value	Gompertz	Logistic
L_0	2.5	2.51	2.35
L_{max}	9.0	9.23	9.11
K	1.0	1.29	1.26
λ	2.5	3.06	2.94

is the shapes of the first derivatives of Eq. 6.2 (Figure 6.2). The peak of each curve of the first derivative is actually the specific growth rate for each model. For the modified logistic model, the first derivative curve is symmetric with respect to its inflection point M, which is not the case for the modified Gompertz model.

The empirical mathematical models shown in Eq. 6.1 are suitable for describing isothermal growth of microorganisms in foods. It can derive important and sufficient information about the growth parameters (*K* and λ) to estimate the extent of microbial growth if the foods are held under constant temperature conditions.

6.2.1.2 Biologically based growth models

6.2.1.2.1 Baranyi model. The major criticisms of the empirical models are that these models are just curves that closely resemble microbial growth curves. The empirical models lack biological meaning, although two parameters (K and λ) derived from the modified Gompertz and logistic models, namely the lag and exponential phases, can be used to describe two of the most important phenomena of microbial growth.

The Baranyi model is probably one of the earliest models that attempted to describe the fundamental mechanism that drives microbial growth. Baranyi (1995) hypothesized that the growth of microorganisms was controlled by their physiological state, which was affected by the prior history, and the duration of the lag phase was controlled by the formation and accumulation of critical substances. Based on these assumptions, the differential equation for microbial growth can be expressed as

$$\frac{d}{dt}C = \alpha(t)\mu(C)C \qquad \text{Eq. 6.5}$$

In Eq. 6.5, C is the actual concentration of microorganisms; $\alpha(t)$ is called the adjustment function, which is a function of time and varies between 0 and 1; and $\mu(C)$ is the potential specific growth rate. The product of $\alpha(t)$ and $\mu(C)$ represents the actual specific rate (Baranyi, McClure, et al., 1993; Baranyi and Roberts, 1994; Baranyi, Roberts, and McClure, 1993). In Baranyi and Roberts (1994) and Baranyi et al. (1995), the definitions of $\alpha(t)$ and $\mu(C)$ were further clarified, and a new term, $\mu(t)$, was used to represent the product of these two terms:

$$\mu(t) = \alpha(t)\mu(C) = \mu_{max}\frac{q(t)}{1+q(t)}\left(1-\frac{C}{C_{max}}\right), \qquad \text{Eq. 6.6}$$

where $q(t)$ is related to the formation and accumulation of critical substances, which are governed by Michaelis-Menten kinetics (Baranyi et al., 1995), and C_{max} is the maximum cell concentration. With this definition, the differential equation for microbial growth becomes

$$\begin{aligned}\frac{dq}{dt} &= \nu q \\ \frac{dC}{dt} &= \mu_{max}\frac{q}{1+q}\left(1-\frac{C}{C_{max}}\right)C\end{aligned} \qquad \text{Eq. 6.7}$$

Using y to denote the natural logarithm of C, and assuming that ν is a constant, Eq. 6.7 can be solved analytically, and the most recent Baranyi model takes the form of

$$y(t) = y_0 + \mu_{max} A(t) - \ln\left[1 + \frac{e^{\mu_{max} A(t)} - 1}{e^{y_{max} - y_0}}\right], \quad \text{Eq. 6.8}$$

where

$$A(t) = t + \frac{1}{\nu}\ln\left(e^{-\nu t} + e^{-h_0} - e^{-\nu t - h_0}\right). \quad \text{Eq. 6.9}$$

In this equation, μ_{max} is termed as the maximum growth rate to differentiate it from specific growth rate K used in other equations. The value of μ_{max} is equal to 2.303 × K, the specific growth rate expressed as the $\log_{10}$ of the microbial count per unit time. To simplify the equation, it is further assumed that $\nu = \mu_{max}$, and $A(t)$ is then actually defined by

$$A(t) = t + \frac{1}{\mu_{max}}\ln\left(e^{-\mu_{max} t} + e^{-h_0} - e^{-\mu_{max} t - h_0}\right) \quad \text{Eq. 6.10}$$

The final Baranyi growth model becomes

$$y(t) = y_0 + \mu_{max} t + \ln\left(e^{-\mu_{max} t} + e^{-h_0} - e^{-\mu_{max} t - h_0}\right) - \ln\left(1 + \frac{e^{\mu_{max} t - h_0} - e^{h_0}}{e^{y_{max} - y_0}}\right). \quad \text{Eq. 6.11}$$

In Eq. 6.11, h_0 is a transformation of q at the time of inoculation, which is calculated from

$$h_0 = -\ln\left(\frac{q_0}{q_0 + 1}\right) = -\ln(\alpha_0). \quad \text{Eq. 6.12}$$

According to Baranyi and Roberts (1994), the lag phase of a growth curve under an isothermal condition can be calculated from

$$\lambda = \frac{h_0}{\mu_{max}}. \quad \text{Eq. 6.13}$$

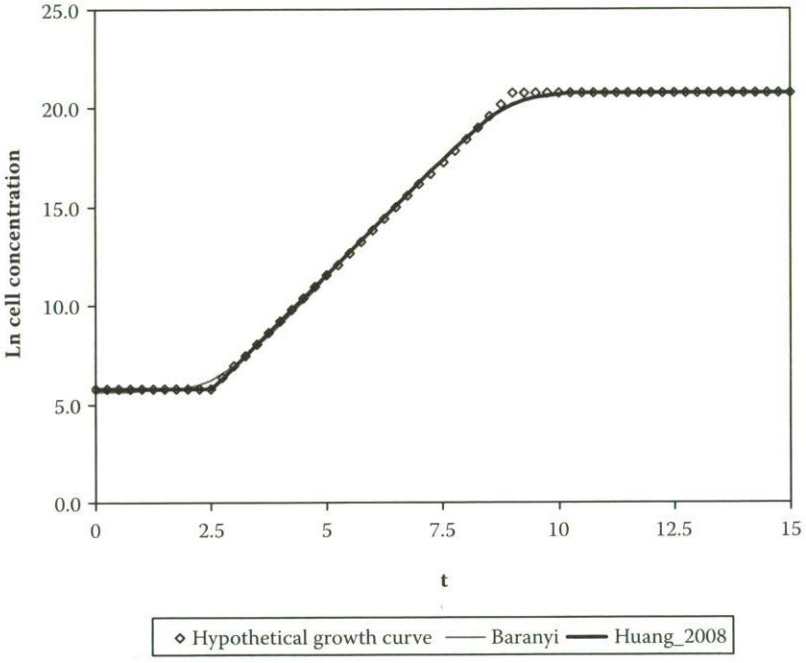

Figure 6.3 Comparison between Baranyi and Huang models used to fit the hypothetical growth curve shown in Figure 6.1.

Nonlinear regression is used to obtain the parameters included in the Baranyi model (Eq. 6.11). Since h_0 defines the initial physiological state of the microorganism, this value may vary from curve to curve. As a result, a mean of h_0 values of different curves (either at the same temperature or under different temperature conditions) is calculated after the first round of curve fitting. A second round of curve fitting is performed again to obtain μ_{max} and λ using the mean h_0 value for each curve. Figure 6.3 shows the fitting of the hypothetical growth (Figure 6.1) using the Baranyi model.

6.2.1.2.2 Huang Model

Based on the three-phase growth phenomenon, Huang (2008) developed a new model that includes a transition function and logistic kinetics to directly define the lag, exponential, and stationary phases. The derivative form of the model takes the form of

$$\frac{dC}{dt} = kC\left(C_{max} - C\right) f\left(\lambda\right), \qquad \text{Eq. 6.14}$$

where

$$f(\lambda)=\frac{1}{1+\exp\left[-\alpha(t-\lambda)\right]}.$$

In Eq. 6.14, the term $f(\lambda)$ is a transition function that defines the duration of the lag phase. This function has a unique mathematical property, with its value ranging from 0 to 1. Within the lag phase, $f(\lambda)$ is zero. Outside the lag phase, $f(\lambda)$ is 1.0. This function helps define the fact that no growth should be observed within the lag phase. After the lag phase, the microbial growth would follow the simple logistic rule with C_{max} as the carrying capacity. The constant α, which is different from $\alpha(t)$ in the Baranyi model, defines the rate of transition from the lag phase to the exponential phase. This value was fixed at 25 in Huang (2008) to ensure a smooth and rapid transition from the lag phase to exponential phase. This differential equation can be solved analytically, and the resulting equation is

$$y(t)=y_0+y_{max} \qquad \text{Eq. 6.15}$$
$$-\ln\left\{\exp(y_0)+\left[\exp(y_{max})-\exp(y_0)\right]\exp\left[-k\exp(y_{max})B(t)\right]\right\},$$

where

$$B(t)=t+\frac{1}{\alpha}\ln\frac{1+\exp\left(-\alpha(t-\lambda)\right)}{1+\exp(\alpha\lambda)}.$$

The definition of $y(t)$ is the same as it is in the Baranyi model. The maximum growth rate is defined by

$$\mu_{max}=kC_{max}. \qquad \text{Eq. 6.16}$$

With this definition, Eq. 6.15 becomes

$$y(t)=y_0+y_{max} \qquad \text{Eq. 6.17}$$
$$-\ln\left\{\exp(y_0)+\left[\exp(y_{max})-\exp(y_0)\right]\exp\left[-\mu_{max}B(t)\right]\right\}.$$

Figure 6.3 also shows the fitting of the Figure 6.1 hypothetical growth curve. The performance of the Huang model is almost identical to the

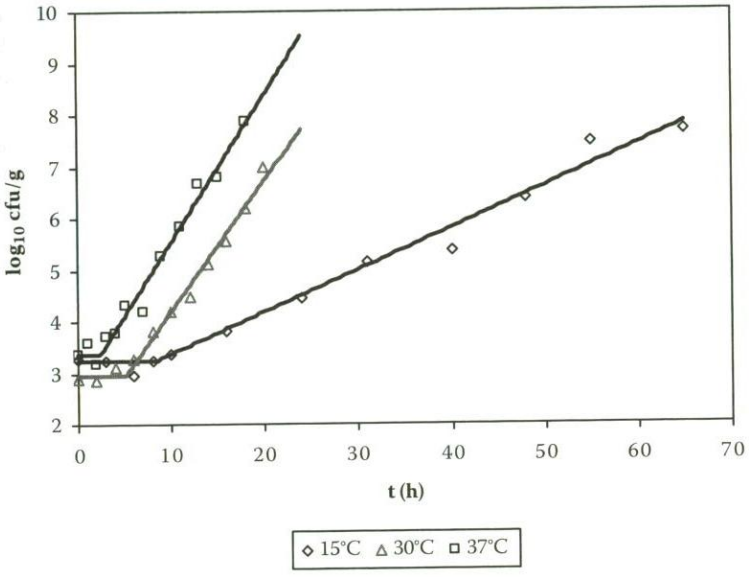

Figure 6.4 Using the reduced Huang model to describe growth curves without stationary phases (Huang 2008).

Baranyi model in the exponential and stationary phases since both models employ the competitive logistic rule for these two phases of microbial growth. However, the Huang model clearly has a more distinctive and mathematically identifiable lag phase than the Baranyi model.

The experimental data reported in Huang (2008) using the Huang model suggested that the duration of a lag phase is not affected by the initial concentration of bacteria. Under an isothermal condition, bacteria remain dormant in the lag phase, after which they enter the exponential phase of growth.

Due to the unique definition of the transitional function used in the Huang (2008) model, it is possible to use the same model to fit growth curves without the stationary phase (Figure 6.4). For this special case, the Huang model can be reduced to

$$y(t) = y_0 + k_{\max}\left\{t + \frac{1}{\alpha}\ln\frac{1+\exp\left[-\alpha(t-\lambda)\right]}{1+\exp(\alpha\lambda)}\right\}. \qquad \text{Eq. 6.18}$$

6.2.1.2.3 Huang 2004 approach

Since *C. perfringens* may exist as spores in RTE meats, the spores must germinate and outgrow before an increase in the number of the *C. perfringens*

can be observed. It is assumed that not all spores germinate at the same time and some spores may germinate faster than others. The germinated spores begin to outgrow and actively divide until the number of cells increases to the maximum capacity, which is also governed by the logistic rule. The number of cells does not begin to increase during the germination and outgrowth of *C. perfringens* spores, which corresponds to the lag phase of the growth process. Mathematically, the cells are either in the state of dormancy or in the state of active dividing. According to Juneja et al. (2001), Juneja and Marks (2003), and Huang (2004), the germination, outgrowth, and growth of *C. perfringens* spores can be described by a set of two differential equations:

$$\frac{dC_L}{dt} = -K_L C_L$$
$$\frac{dC_D}{dt} = -\frac{dC_L}{dt} + K_D C_D \left(1 - \frac{C_D}{C_{Max}}\right) \qquad \text{Eq. 6.19}$$

In Eq. 6.19, C_L represents the concentration of *C. perfringens* cells in the state of dormancy, and C_D is the concentration of cells that are actively dividing. This equation also suggests that the dormant cells leave the state of dormancy following the first-order kinetics. After the cells leave the state of dormancy, they begin to actively divide. Apparently, C_L is equal to the initial concentration of the inoculums. For *C. perfringens* spores, C_D is equal to zero at the time of inoculation. At any given time, the number of cells recoverable from the food includes the cells in the state of dormancy and the cells that are actively dividing. Therefore, the total concentration of cells (C) recoverable from the food can be calculated from

$$C = C_L + C_D \qquad \text{Eq. 6.20}$$

According to Eq. 6.19, the increase in the number of actively dividing cells is affected by both the rate at which the cells leave the state of dormancy and the rate at which the cells actively divide. To solve this equation for fitting an isothermal growth curve, it is necessary to determine both K_L and K_D. To simplify the problem, it is assumed that K_L is a fraction of K_D (Huang, 2004), and the relationship between K_L and K_D becomes

$$K_L = \alpha K_D \qquad \text{Eq. 6.21}$$

With Eq. 6.21, the differential growth equation can be written as

$$\frac{dC_L}{dt} = -\alpha K_D C_L$$
$$\frac{dC_D}{dt} = -\frac{dC_L}{dt} + K_D C_D \left(1 - \frac{C_D}{C_{Max}}\right) \qquad \text{Eq. 6.22}$$

Within the limits of temperatures suitable for microbial growth, α ranges between 0 and 1; that is, $0 \le \alpha \le 1$. If $\alpha = 0$, all the cells would remain in the state of dormancy and never enter the state of active division. The cell concentration would remain constant and is equal to the concentration of cells initially inoculated into the food. If $\alpha = 1$, then all the initially inoculated cells would immediately enter the state of active division. In Huang (2004) and Juneja et al. (2006), α was fixed at 0.01 when this model was used to fit the growth curves of *C. perfringens* in cooked meats. It is necessary to mention that K_D in Eq. 6.19 or 6.22 is equivalent to μ_{max} in the Baranyi model or Huang model, which is equal to $2.303 \times K$.

The duration of the lag phase of an isothermal growth process is not explicitly expressed in Eq. 6.22. However, the duration of the lag phase during an isothermal process can be calculated from (Huang, 2004; Juenja and Marks, 2002):

$$\lambda = \frac{\ln\left(1 + \frac{K_D}{K_L}\right)}{K_D} = \frac{\ln\left(1 + \alpha^{-1}\right)}{K_D} \qquad \text{Eq. 6.23}$$

Eq. 6.22 is an initial value problem that cannot be solved analytically, but can be easily solved using a numerical method (Huang, 2004); this will be discussed in more detail in Section 6.3 of this chapter. Figure 6.5 shows the results of numerical analysis to solve Eq. 6.22 used to fit the hypothetical growth curve shown in Figure 6.1. The specific growth rate determined from solving the different equations (Eq. 6.22) is 1.06 $\log_{10}$ per unit time, and the duration of the lag phase is 2.48. Both the specific growth rate and lag phase are almost identical to the values specified in Figure 6.1. Another advantage of the Huang 2004 approach is that it also can be used to fit growth curves without stationary phase (Juneja et al., 2006).

6.2.2 *Secondary models and the effect of temperature*

The effect of temperature on microbial growth is primarily manifested in the changes in the growth rate and the lag phase duration as the growth temperature varies. Generally, microorganisms would grow within the lower limit (T_{min}) and the upper limit (T_{max}) of the temperature. At the

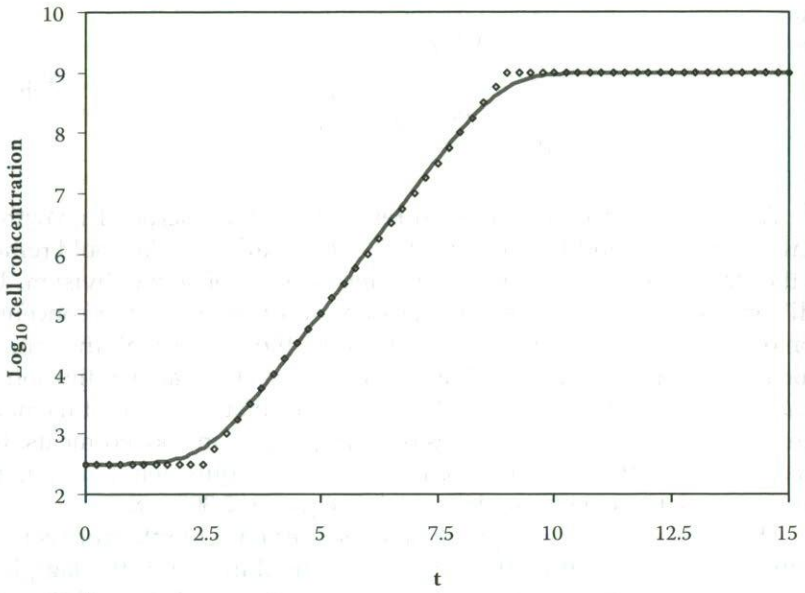

Figure 6.5 Using the two-stage differential growth model to fit the hypothetical growth curve shown in Figure 6.1 (Huang, 2004).

optimum temperature (T_{opt}), the microbial growth would exhibit the highest growth rate and the lowest lag phase duration. Microorganisms cannot grow at temperatures below T_{min} or above T_{max}. At temperatures between T_{min} and T_{opt}, the growth rate would generally increase and the duration of lag phase would decrease with temperature. As the temperature increases above T_{opt}, the microbial growth would generally slow down. Although many secondary models have been developed to describe the effect of temperature on microbial growth, the most widely used and the most practical secondary model is probably the Ratkowsky model, which is written as

$$K_{max}(T)^{\delta} = \beta_1 (T - T_{min})^{2\delta} \left\{1 - \exp\left[\beta_2 (T - T_{max})\right]\right\} \qquad \text{Eq. 6.24}$$

The δ value in Eq. 6.24 can be 0.5 or 1.0. If δ is 0.5, then Eq. 6.24 is the traditional Ratkowsky model, more commonly known as the square-root model (Ratkowsky et al., 1983). If δ is 1.0, then Eq. 6.24 becomes a modified Ratkowsky model (Zwietering et al., 1991), which is a variant of the original square-root model. The coefficients β_1 and β_2 define the rate at which K_{max} responds to temperature.

The lag phase duration usually changes inversely with K_{max}. Therefore, the Ratkowsky model can also be used to describe the changes in λ as a function of temperature (Eq. 6.26; Juneja and Marks, 1999; Juneja et al., 1999; Zwietering et al., 1991).

$$\lambda^{-\delta} = \beta_1 \left(T - T_{min}\right)^{2\delta} \left\{1 - \exp\left[\beta_2 \left(T - T_{max}\right)\right]\right\} \qquad \text{Eq. 6.25}$$

Although Eq. 6.24 and Eq. 6.25 are empirical in nature, it is one of the best models for describing the effect of temperature on the growth of microorganisms in foods. The T_{min} and T_{max} estimated by the Ratkowsky model can be very close to the biological limits of temperature for microorganisms in foods (Ratkowsky et al., 1982; Ratkowsky et al., 1983).

6.2.2 *Tertiary model*

A tertiary model is a mode that relates both intrinsic and extrinsic conditions to the growth parameters. Common intrinsic factors include pH, fat content, water activity, and concentrations of certain ingredients that affect the growth of microorganisms. For *C. perfringens*, Juneja et al. (1996) developed a comprehensive model to describe the effect of temperature, pH, sodium chloride, and sodium pyrophosphate on the generation time and growth rate of *C. perfringens* in a model food system.

6.3 *Methods and models for growth under dynamic conditions*

Under a dynamic condition, temperature changes with time, and so does the rate constant. Therefore, it is necessary to combine a primary model with a secondary model to estimate the growth of microorganisms under dynamic temperature conditions. The differential forms of the Baranyi model (Eq. 6.7), Huang model (Eq. 6.14), and Huang 2004 model (Eq. 6.22) can be directly used to estimate the dynamic growth of microorganisms. The empirical primary models, however, cannot be directly used in a dynamic temperature condition. A transformation of the modified Gompertz and logistic equations is needed. To transform the empirical models, a first derivative of Eq. 6.1 must be taken, resulting in

$$\frac{dL}{dt} = \begin{cases} \mu\left(L - L_0\right) \ln\left(\dfrac{L_{max} - L_0}{L - L_0}\right) & \textit{Gompertz} \\ \mu\left(L - L_0\right) \dfrac{\left(L_{max} - L\right)}{L_{max} - L_0} & \textit{Logistic} \end{cases} \qquad \text{Eq. 6.26}$$

Since the rate constant changes with temperature, all differential forms of the growth models cannot be solved directly by analytical methods, but they can be easily solved using proper numerical methods. Although many numerical methods can be used to solve differential equations, the Runge-Kutta method remains a method of choice for solving differential growth equations to estimate the growth of microorganisms under dynamic temperature conditions. This method is a standard method for solving differential equations and is discussed in more detail in many textbooks; however, a brief introduction of the fourth-order Runge-Kutta method is given here (Chandra and Singh, 1995).

Denoting $f(x, t)$ as a general differential equation for the growth model:

$$\frac{dx}{dt} = f(x,t), \qquad \text{Eq. 6.27}$$

where x is L or C in Eqs. 6.7, 6.14, 6.22, or 6.26, and t is the growth time.

The Runge-Kutta method is based on the previous value and a small increment in the independent variable to solve an initial value problem. For growth models, the independent variable is time. To use the Runge-Kutta method, the time domain is first divided into small segments of equal length, with each segment equal to $h = t/n$, where n is the number of segments. To estimate the value of x, the Runge-Kutta method first calculates four coefficients based on the previous value:

$$\begin{aligned} k_1 &= hf\left(t_{i-1}, x_{i-1}\right) \\ k_2 &= hf\left(t_{i-1} + \frac{h}{2}, x_{i-1} + \frac{k_1}{2}\right) \\ k_3 &= hf\left(t_{i-1} + \frac{h}{2}, x_{i-1} + \frac{k_2}{2}\right) \\ k_4 &= hf\left(t_{i-1} + h, x_{i-1} + k_3\right) \end{aligned} \qquad \text{Eq. 6.28}$$

where i is the i^{th} point of time ($i = 1$ to n). These four coefficients are then used to calculate the value of x_i at the $t = t_i$:

$$x_i = x_{i-1} + \frac{1}{6}\left(k_1 + 2k_2 + 2k_3 + k_4\right) \qquad \text{Eq. 6.29}$$

The Runge-Kutta method can be implemented using any computing language, even in a spreadsheet such as Microsoft Excel. In each growth

model, there is a rate constant. For the modified Gompertz and logistic model, the relative growth rate μ should be used.

In a dynamic process, the temperature changes with time. Therefore, the rate constant is an implicit function of time. Let $T = g(t)$, then the rate constant can be expressed as a function of time, which is

$$K_{\max}\left(g\left(t\right)\right)=\beta_1\left(g\left(t\right)-T_{\min}\right)^2\left\{1-\exp\left[\beta_2\left(g\left(t\right)-T_{\max}\right)\right]\right\} \quad \text{Eq. 6.30}$$

With a known initial value of microbial concentration, the dynamic growth equation can be successfully solved (Huang, 2003, 2004; Juneja et al., 2006).

6.4 *Heat transfer and transient temperature history*

As a product cools after cooking, the temperature of the food changes continuously. This is an unsteady state heat transfer process. To estimate the potential growth of *C. perfringens* in cooked meats during cooling, it is necessary to have an accurate temperature history at the slowest cooling point, which is usually the geometric center of the RTE meats. Several methods can be used to obtain the temperature history at the geometric center of a solid food. The most accurate method is to directly measure the temperature history at the geometric center. The second method is to estimate the temperature history using the starting and ending temperatures at the geometric center. Another method is to estimate the temperature history by computer simulation based on the physical properties of the food and environmental conditions. Due to the limitations of this book, it is impossible to discuss all these methods in detail, but a brief introduction to each of these methods is given in this chapter.

6.4.1 *Direct measurement of temperature*

With the advancement of measurement and data acquisition technologies, it is now relatively easy to measure the temperature of meats during cooling. Many types of data-loggers are commercially available. Modern data-loggers are sufficiently rugged, miniaturized, and can be attached and moved with cooked meats. Table 6.2 lists some of the websites of the manufacturers of data-loggers.

The most widely used transducers for measuring temperature are probably thermocouples that can be directly inserted into cooked meats. For the temperature range experienced during cooling of cooked meats,

Table 6.2 Lists of Models and Manufacturers of Data-Loggers

Model	Manufacturer/Distributor
OM-DAQPRO-5300	Omega Engineering (www.omega.com)
iTCX-W	
OM-CP-BRIDGE110-10	
OM-CP-EVENT101	
OM-CP-HITEMP-150	
OM-CP-HITEMP-150FP	
OM-CP-LEVEL101-SS	
OM-CP-OCTTEMP	
OM-CP-QUADTEMP	
OM-CP-TCTEMP1000	
OM-CP-THERMOVAULT	
HOBO U12 Stainless Steel Temperature **(U12-015)**	MicroDAQ.com, Ltd (www.microdaq.com)
HOBO U12 Temp Logger w/5-in Stainless Probe **(U12-015-02)**	
Advantech Data Acquisition I/O Module	Cole-Parmer (www.coleparmer.com)
Model K-18808-06, K-18808-08	
Cole-Parmer Temperature Datalogger	
Model K-38010-15	

Type-T thermocouple probes are probably the most suitable and accurate for measuring temperature changes. To accurately measure the temperature of cooked meats at the geometric center, it is necessary to choose a thermocouple probe that is small but strong enough to penetrate into the center of the meat. However, it is also important to ensure that the section of the probe inserted into the meat is 10 to 15 times longer than the diameter of the probe to prevent the conduction of the heat through the metal sheath to the tip of the probe.

6.4.2 *Estimation by start and end points of temperature*

When a direct measurement of temperature is technically infeasible, one may try to use the starting and end-point temperatures to estimate the temperature history of cooked meats. To use this method, one assumes that the temperature of the product changes exponentially with time. However, this method is the least accurate method for thermally conductive foods such as cooked meats, and it only works under certain physical conditions. In general, this method is also known as the lumped-capacitance method

when the internal resistance to heat transfer is negligible (Inpcropera and DeWitt, 1996; Singh, 1992) and is based on the balance of heat energy during cooling. Assuming that the temperature of the product is uniformly distributed at the start of cooling, the transfer of heat to the food is governed by (Inpcropera and DeWitt, 1996; Juneja et al., 1994)

$$-h_s A\left(T-T_\infty\right)=\rho V C_p \frac{dT}{dt} \qquad \text{Eq. 6.31}$$

In Eq. 6.31, h_s is the surface heat transfer coefficient (W/m^2·°C), A is the surface area (m^2), T_∞ is the ambient temperature (°C), ρ is density (kg/m^3), V is the volume (m^3), and C_p is the heat capacity (J/kg·°C). Denoting T_0 as the initial temperature, this equation can be integrated to produce

$$\frac{T-T_\infty}{T_0-T_\infty}=\exp\left[-\frac{h_s A}{\rho V C_p}t\right] \qquad \text{Eq. 6.32}$$

Eq. 6.32 is more conveniently expressed as two important dimensionless numbers in engineering—the Biot number and the Fourier number:

$$Bi=\frac{h_s L_c}{k}$$
$$Fo=\frac{\alpha t}{L_c^{\,2}} \qquad \text{Eq. 6.33}$$

In Eq. 6.33, L_c is the characteristic length of an object, which is half of the thickness of a plane, half of the radius of a long cylinder, or one-third of the radius of a sphere, and α is the thermal diffusivity of the product (W/m °C). The accuracy of the lump-capacitance model is highly dependent on the Biot number. In general, the Biot number must be < 0.1 for the lamp-capacitance model (Inpcropera and DeWitt, 1996).

The coefficient terms in Eq. 6.32 also can be used to calculate the thermal time constant, τ, which is equal to $(\rho V C_p)/(h_s A)$. Therefore, the lump-capacitance model also can be expressed as

$$\frac{T-T_\infty}{T_0-T_\infty}=\exp\left(-\frac{t}{\tau}\right). \qquad \text{Eq. 6.34}$$

According to Eqs. 6.33 and 6.34, only under a special condition can the starting and end-point temperatures be used to estimate the temper-

ature history of cooked meats during cooling. The first condition is that the temperature is uniform at the initiation of the cooling process. The second condition is that the Biot number is < 0.1. The third condition is that the thermal time constant is equal to the total cooling time (*t_cool*). Under these strict physical conditions, the starting and end-point temperatures can be used to estimate the cooling history with reasonable accuracy:

$$T = T_\infty + (T_0 - T_\infty) \exp\left(-\frac{t}{t\_cool}\right) \qquad \text{Eq. 6.35}$$

6.4.3 *Computer simulation of the cooling process*

The entire history of cooking and cooling of meat products can be described by the physical laws governing the process of heat transfer. The transient heat transfer process during cooking and cooling of meats is basically a heat conduction problem with convective boundary conditions. Computer simulation can be used to solve this type of problem with relative ease. Including the cooking (heating) process in the simulation is actually beneficial to solving the heat transfer problem and obtaining a more accurate temperature history at the geometric center of cooked meats during cooling. The reason is that the transient heat transfer process during cooling is also an initial value problem. The accuracy of a computer simulation depends on the accurate definition of the initial conditions of a heat transfer process. At the end of cooking and the starting of cooling, it is very difficult to obtain the temperature distribution within the cooked products, and it is highly unlikely in the real world that the temperature would be evenly distributed. By simulating the heating process together with the cooling of cooked products, it is possible to obtain a more accurate temperature history during cooling. The transient heat transfer during cooking and cooling of meats can be described by a general partial differential equation in Cartesian coordinates (Incropera and DeWitt, 1996):

$$\frac{\partial T}{\partial t} = \frac{k}{\rho C_p}\left(\frac{\partial^2 T}{\partial x^2} + \frac{\partial^2 T}{\partial y^2} + \frac{\partial^2 T}{\partial z^2}\right) \qquad \text{Eq. 6.36}$$

In Eq. 6.36, k is the thermal conductivity of the product (W/m °C); ρ and C_p are density and heat capacity; and x, y, and z are the coordinates of any location in the product. For most meat products, the changes in the physical properties can be considered negligible during cooking or cooling. The initial condition of this partial differential equation is $T(x, y, z) = T_0(x, y, z)$, which is the temperature profile before cooking or cooling starts. The boundary conditions for this equation are

$$-k\frac{\partial T}{\partial \vec{n}} = h\left(T - T_{\infty}\right) + w_e L_v \qquad \text{Eq. 6.37}$$

Eq. 6.37 describes the convection of heat to the surface of meats and the flux of thermal energy caused by evaporative loss. The terms w_e and L_v are rate of moisture evaporation (kg/m²s) and latent heat (J/kg). Eq. 6.36 can be used to describe heat transfer in a three-dimensional system of any geometrical shapes. Many real foods have a much simpler geometry. If heat is conducted along one direction, the heat transfer equation can be simplified to

$$\frac{dT}{dt} = \frac{k}{\rho C_p}\frac{d^2T}{dx^2} \qquad \text{Eq. 6.38}$$

For cylindrically shaped foods, the heat transfer equation becomes

$$\frac{dT}{dt} = \frac{k}{\rho C_p}\left(\frac{d^2T}{dr^2} + \frac{1}{r}\frac{dT}{dr}\right) \qquad \text{Eq. 6.39}$$

For a spherical food, the heat transfer equation becomes

$$\frac{dT}{dt} = \frac{k}{\rho C_p}\left(\frac{d^2T}{dr^2} + \frac{2}{r}\frac{dT}{dr}\right) \qquad \text{Eq. 6.40}$$

6.5 *Numerical analysis of heat transfer*

With the advancement of modern computing technology, the heat transfer equation can be routinely solved by numerical methods. The most frequently used numerical methods for solving the unsteady state heat transfer equations are finite difference methods and finite element methods (Chandra and Singh, 1995; Sheen and Hayakawa, 1991; Sheen et al., 1993). Huang (2007) developed an approach to simultaneously determine the surface heat transfer coefficient and thermal diffusivity using an implicit finite difference method. This method can be directly used to simulate the process of heating and cooling of meat products. Many commercial packages for solving heat transfer partial differential equations are also available. One example of such products is FlexPDE (http://www.pdesolutions.com), a finite element package capable of solving 3-D partial differential equations.

Solving transient heat transfer equations requires accurate data of physical properties. It is desirable to directly measure the physical

properties of meat products. However, for most meat products, the thermal diffusivity is around 1.2 ~ 1.4 × 10^{-7} m^2/s. The density of meats is very close to water, and the thermal conductivity ranges between 0.4 and 0.5 W/m °C. The heat capacity is around 3.56 to 3.77 kJ/kg °C for beef meat and 3.62 kJ/kg °C for broilers (Rahman, 1996).

6.6 *Practical applications of growth models and dynamic simulation*

6.6.1 *Primary and secondary models*

All primary models, except the more recently developed Huang model, have been used to describe the growth of *C. perfringens* in cooked meats under temperature conditions applicable to cooling. Juneja et al. (1999) investigated the growth of *C. perfringens* in a broth system (trypticase-peptone-glucose-yeast extract) at different temperatures and developed a secondary model to describe the exponential growth rate (K) and lag phase duration (λ) as a function of temperature.

$$K^{\frac{1}{2}} = 0.044(T - 10.13)\left\{1 - \exp\left[0.419(T - 51.02)\right]\right\}^{\frac{1}{2}} \quad \text{Eq. 6.41}$$

$$\lambda^{\frac{1}{2}} = 0.020(T - 10.13)\left\{1 - \exp\left[0.190(T - 51.02)\right]\right\}^{\frac{1}{2}} \quad \text{Eq. 6.42}$$

Juneja et al. (2001) studied the growth of *C. perfringens* in irradiated ground beef (15% fat) and used Eq. 6.19 to solve growth curves without the stationary phase; they subsequently developed a secondary model for the exponential growth rate:

$$K^{\frac{1}{2}} = 0.035(T - 11.18)\left\{1 - \exp\left[0.231(T - 51)\right]\right\}^{\frac{1}{2}} \quad \text{Eq. 6.43}$$

Using the same approach, Juneja and Marks (2002) continued to investigate the growth of *C. perfringens* in cured chicken, and developed a model to estimate the growth rate as a function of temperature:

$$K^{\frac{1}{2}} = 0.0358(T - 12.3)\left\{1 - \exp\left[0.201(T - 51)\right]\right\}^{\frac{1}{2}} \quad \text{Eq. 6.44}$$

The growth differential equation (Eq. 6.19) also was solved using the Runge-Kutta method (Huang 2004 approach) to fit the complete growth curves (including all three phases) of *C. perfringens* in 93% lean cooked ground beef (Huang 2004), and the resulting secondary equation is

$$K_D = 0.003187(T - 9.11)^2 \left\{1 - \exp\left[0.5446(T - 51.21)\right]\right\} \quad \text{Eq. 6.45}$$

The Huang 2004 approach also was used to fit the growth curves obtained from cooked cured pork (Juneja et al., 2006). The secondary model for *C. perfringens* in cooked cured pork is

$$K = 0.00243(T - 13.5)^2 \left\{1 - \exp\left[0.41(T - 50.6)\right]\right\} \quad \text{Eq. 6.46}$$

The Baranyi model was used by Amezquita et al. (2005) to fit the growth curves of *C. perfringens* in cooked boneless ham. The original Ratkowsky square-root model was used to describe the growth of *C. perfringens* as a function of the absolute temperature, which is expressed as

$$\sqrt{k_{\max}} = 0.0599(T_K - 283.9) \quad \text{Eq. 6.47}$$

Juneja et al. (2008) also used the Baranyi model to fit the growth curves in *C. perfringens* in cooked uncured beef, resulting in

$$K^{\frac{1}{2}} = 0.0504(T - 10.15)\left\{1 - \exp\left[0.238(T - 52.98)\right]\right\}^{\frac{1}{2}} \quad \text{Eq. 6.48}$$

All the secondary models for exponential growth rate K suggested that the minimum growth temperature for *C. perfringens* in cooked meats is around 10°C to 14°C, which is the minimal temperature range for growth of *C. perfringens*. All secondary models, except Eq. 6.47, suggest that the maximum growth temperature for *C. perfringens* in cooked meats is between 51°C and 53°C. The optimum growth temperature is located between 45°C and 48°C, according to Figure 6.6, which is also agreeable with the data reported in the literature (Craven, 1980). In general, the growth rate of *C. perfringens* in cured meats is about one-third to one-half of the growth rate found in uncured meats (Figure 6.6).

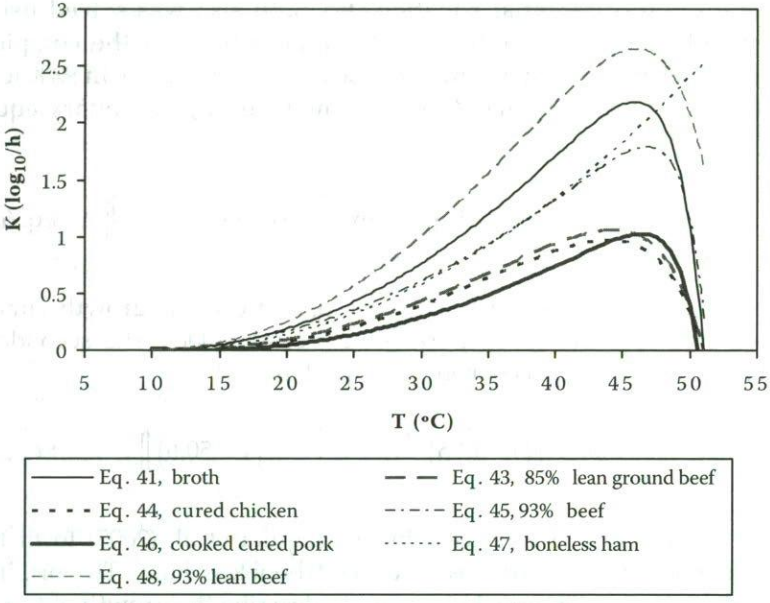

Figure 6.6 The exponential growth rate (K) as a function of temperature and described by the Ratkowski models.

6.6.2 *Dynamic simulation of* C. perfringens *growth*

6.6.2.1 *FlexPDE as a simulation package*

Although a few papers have been published on dynamic simulation of growth of *C. perfringens* in cooked meats (e.g., Amezquita, Wang, and Weller, 2005; Huang, 2004), computer codes used for computation were specially developed. The computer program developed by Huang (2004) was based on Visual Basic Professional Version 6 (Microsoft, Redmond, WA). The program can simulate the growth of *C. perfringens* in cooked meats under both dynamic and isothermal conditions, but it does not have the capability to simulate the heat transfer process during cooking or cooling. The computational codes developed by Amezquita et al. (2005) were an integrated model capable of simulating the temperature history of cooked meats and the growth of *C. perfringens*. A finite element method was used by heat transfer during heating and cooling of boneless ham (Amezquita, Wang, and Weller, 2005). The computer program was based on a computational platform Matlab Version 6.5 (The Mathworks, Inc., Natick, MA), which requires special programming knowledge and is not a user-friendly computing package.

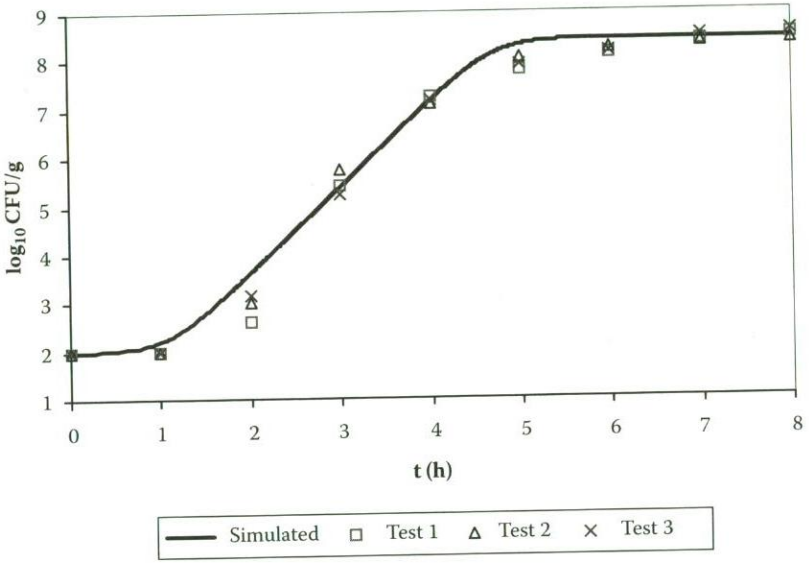

Figure 6.7 Simulation of *C. perfringens* growth in cooked beef at 47°C using Eq. 6.45. The raw data were taken from Huang (2004).

The FlexPDE software is a user-friendly and multi-purpose finite element analysis package capable of simulating complex physical processes. It can also solve ordinary differential equations (ODEs) for bacterial growth. For this reason, this finite element computing package is used in this chapter to demonstrate the dynamic simulation of *C. perfringens* growth in cooked meats.

Figure 6.7 illustrates the simulation of *C. perfringens* growth in cooked beef at 47°C using FlexPDE Version 4.2. The raw data in this figure were taken from Huang (2004), and the growth rate was calculated from Eq. 6.45. Figure 6.8 demonstrates the simulation of the growth of *C. perfringens* in cooked beef cooled exponentially from 51°C to 10°C in 18 h. The simulation results shown in Figures 6.7 and 6.8 duplicated the results previously published by Huang (2004), indicating the FlexPDE is suitable for numerical analysis of growth of *C. perfringens* in cooked meats under both isothermal and dynamic temperature conditions.

6.6.2.2 *Computer simulation of* C. perfringens *growth during dynamic cooling*

As mentioned previously, the accuracy of estimating the growth of *C. perfringens* in cooked meats during dynamic cooling is affected by the secondary growth models and the temperature history at the geometric

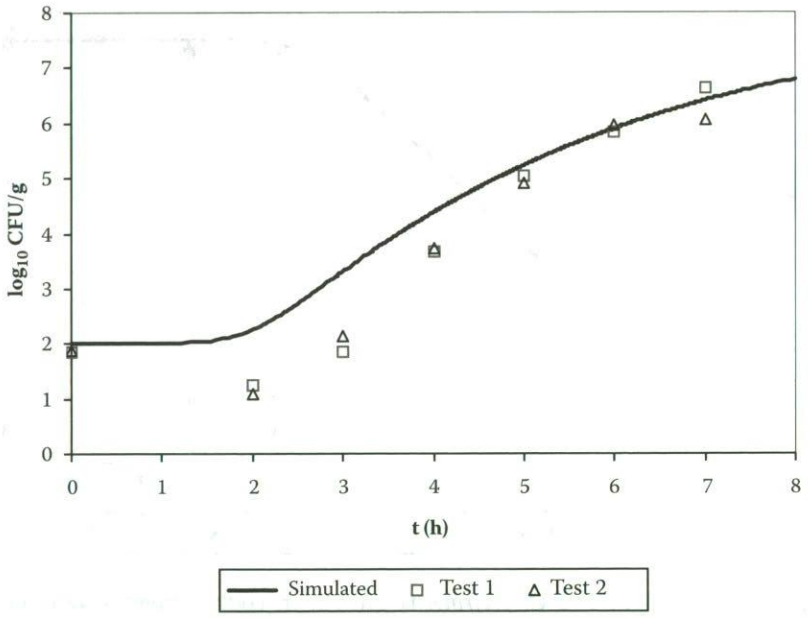

Figure 6.8 Simulation of growth of *C. perfringens* in cooked beef with temperature changing exponentially from 51°C to 10°C in 18 h. The raw data were taken from Huang (2004).

center of the product. If it is possible to physically measure the temperature history of the product, the data can be directly used to simulate the growth of *C. perfringens*. If the temperature history cannot be physically obtained, it is possible to use a computer simulation to simulate the temperature of cooked meats during cooling. If the temperature of a product is not uniformly distributed at the end of cooking, it is necessary to simulate the entire temperature history during both heating and cooling. This is the approach used in this chapter to demonstrate the application of computer simulation to estimate the growth of *C. perfringens* in cooked beef.

FlexPDE is used to simulate the growth of *C. perfringens* in cooked beef using physical examples taken from the literature. The objective of computer simulation was to demonstrate the effect of cooling temperature and heat transfer coefficient during cooling on *C. perfringens* growth in cooked meats. The physical example of cooking is taken from Obuz et al. (2002). Conditions for the cooling process are taken from Amezquita, Wang, and Weller (2005). Physical properties and conditions of the simulated product are listed in Table 6.3. The product is a cylindrically shaped beef roast (0.09 m in diameter and 0.19 m in height). The thermal properties

Table 6.3 Physical Conditions and Thermal Properties Used in Computer Simulation of *C. perfringens* Growth during Cooling

Parameters	Value
Material and Shape[a]	Cylindrical beef roast
Diameter (m)[a]	0.09
Height (m)[a]	0.19
Thermal conductivity (W/m °C)[b]	0.5
Thermal diffusivity (W/s^2)[b]	1.3×10^{-7}
Surface heat transfer coefficient (W/m^2 °C)	
Heating[a]	75
Cooling[c]	10
Rate of evaporation (kg/m^2s)	1.8×10^{-3}
Heating temperature (°C)[a]	163[a]
Cooling ambient temperature (T_a, °C)	1, 5, 10, 15
Heating time (h)[a]	1.5
Cooling time (h)	10

[a] Obuz et al. (2002)
[b] Rahman (1996)
[c] Amezquita, Wang, and Weller (2005)

of the product are taken from Rahman (1996). It was assumed that heat loss through moisture evaporation was negligible during cooling. During cooking, however, it was assumed that moisture evaporated at a rate of 1.8×10^{-3} kg/m^2s. Moisture evaporation was needed to compensate the heating through latent heat, which is calculated from Amezquita, Wang, and Weller (2005).

$$L_v = -2.5 \times 10^3 T + 2.5 \times 10^6 \qquad \text{Eq. 6.49}$$

Both the Baranyi model (Eq. 6.7) and Huang 2004 approach (Eq. 6.19) were used to estimate the growth of *C. perfringens* during cooling. The secondary model was based on Eq. 6.47 (Amezquita et al., 2005) for the Baranyi model and Eq. 6.45 for the Huang 2004 approach. To use Eq. 6.47 during cooling, the upper temperature was set at 51.21°C, the same as the highest temperature used in Eq. 6.45. These two secondary models were chosen because they are very similar. The curves are almost identical at temperatures below 42°C.

To validate the suitability of using FlexPDE to simulate the heat transfer process, it was used to duplicate the heating process described in Figure 6.2 of Obuz et al. (2002). Figure 6.9 shows the temperature histories on the surface and at the geometric center of a cylindrically shaped beef roast. The temperature histories simulated by FlexPDE are similar

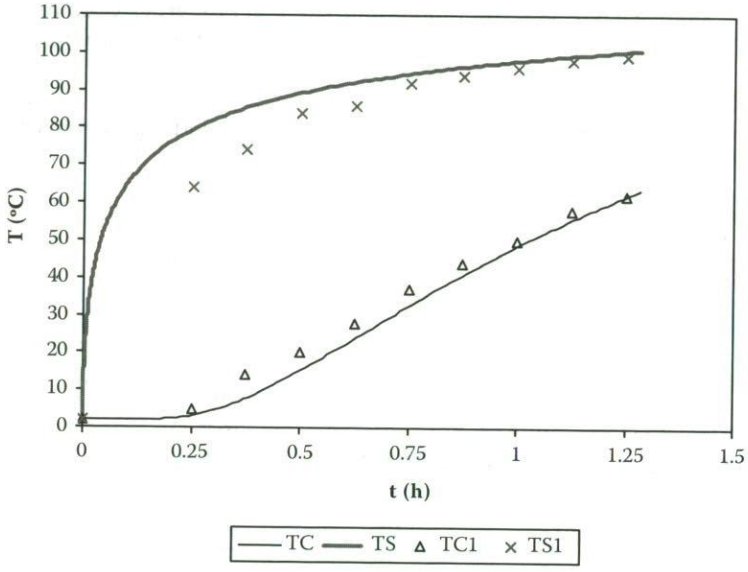

Figure 6.9 Computer simulation of the temperature profiles during cooking a cylindrically shaped beef roast (Diameter = 0.09 m, Height = 0.19 m). TC and TS are temperatures at the geometric center and on the surface of beef roast. TC1 and TS1 are temperature histories at the geometric center and on the surface of beef roast, taken from Figure 6.2 of Obuz et al. (2002). The initial temperature is 2°C. Other physical conditions and properties are listed in Table 6.3.

to the results reported in Figure 6.2 of Obuz et al. (2002), indicating that FlexPDE can be used as a tool to simulate the heat transfer process during the cooking of processed meats, considering the fact that the thermal property data were not directly measured but taken from a reference book (Rahman, 1996).

6.6.2.3 *Scenario 1—Effect of cooling temperature on growth of* C. perfringens

In this example, FlexPDE was used to simulate the temperature histories of a cylindrically shaped beef roast during cooking and cooling. The objective was to evaluate the effect of cooling temperature on the growth of *C. perfringens*. FlexPDE was used to simulate both heating and cooling of the beef roast. The physical conditions for heating and cooling are listed in Table 6.3. In sum, all the beef roasts simulated using FlexPDE underwent the same heating conditions during cooking, and the same heat transfer coefficient (10 W/m^2s) was applied during the cooling. The only difference

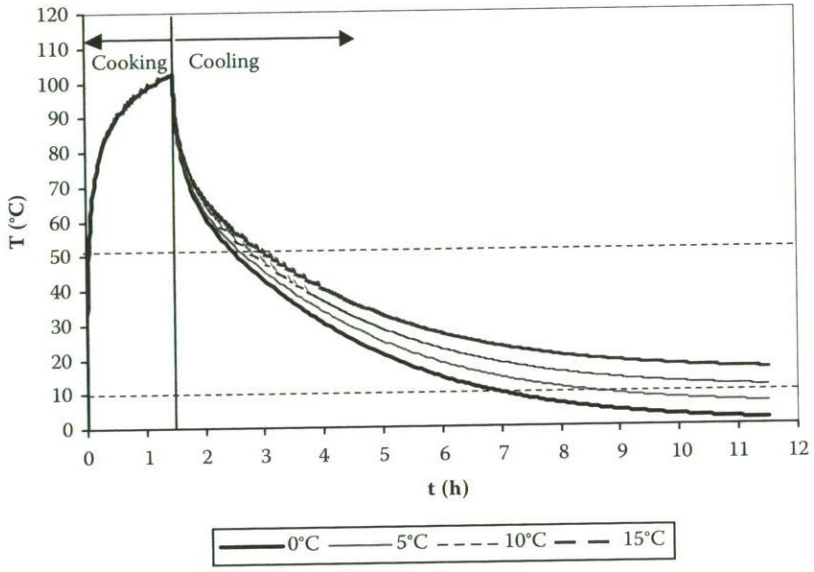

Figure 6.10 Simulated surface temperature histories during cooking and cooling of beef roasts. The legends represent cooling air temperatures. The dotted horizontal lines represent the upper and lower temperature limits. The heat transfer coefficient during cooling was 10 W/m²s.

was the cooling temperature. The initial cell concentration was 2 $\log_{10}$ CFU/g. Figure 6.10 shows the simulated surface temperature histories of beef roast during cooking and cooling. Figure 6.11 shows the temperature histories at the geometric center of the beef roasts. The temperature histories shown in these two figures illustrate that the heating process was indeed the same among all these simulated processes. However, the temperature histories were significantly affected by the cooling air temperature. In general, the surface temperature of the beef roasts began to decrease immediately after cooling started and gradually equilibrated to the cooling air temperatures (Figure 6.10). The center temperatures, however, did not begin to decrease immediately after cooling started. Instead, the center temperatures continued to increase because of the residual heat in the beef roasts at the initial stage of cooling. After the center temperature peaked, it also began to decrease gradually (Figure 6.12). With cooling temperatures of 0°C and 5°C, the center temperatures passed through the "growth zone (between T_{max} and T_{min})" in 4.3 h and 5.6 h, respectively. With cooling temperatures of 10°C and 15°C, the center temperatures of beef roasts were above the minimum growth temperatures during the

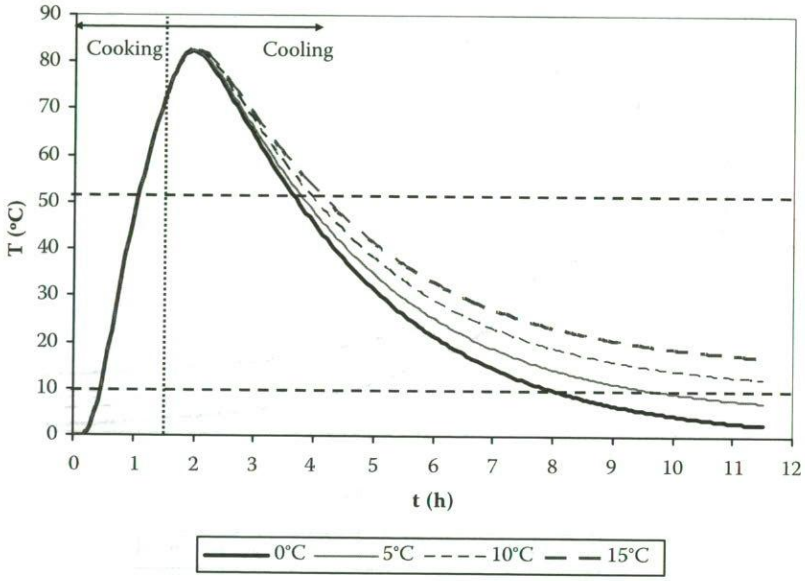

Figure 6.11 Simulated center temperature histories during cooking and cooling of beef roasts. The legends represent center temperatures. The dotted horizontal lines represent the upper and lower temperature limits. The heat transfer coefficient during cooling was 10 W/m²s.

entire 10 h process of cooling. The time needed to pass through the temperature range between 51°C and 27°C was approximately 1.4, 2.0, 2.3, and 2.9 h with cooling air temperatures of 0, 5, 10, and 15°C, respectively.

Figure 6.13 shows the estimated growth of *C. perfringens* in beef roasts during cooling using the Huang 2004 approach. Using this method, the estimated overall growth during the entire 10 h cooling process was 0.03, 0.05, 0.19, and 0.63 logs, corresponding to the cooling temperature maintained at 0, 5, 10, and 15°C, respectively. With the Baranyi model (Figure 6.14), the estimated overall growth of *C. perfringens* in cooked beef roasts was 0.09, 0.19, 0.54, and 1.09 logs, corresponding to cooling at 0, 5, 10, and 15°C. The relative growth estimated by the Huang 2004 approach and the Baranyi model was basically identical at lower cooling temperatures (0°C and 5°C). At higher cooling temperatures (10°C and 15°C), the relative growth estimated by the Baranyi model was slightly higher than that estimated by the Huang 2004 approach. The overestimation by the Baranyi model in the latter cases can be attributed to the incompleteness of the secondary model (Eq. 6.47). Since the secondary model used for the Baranyi model (Eq. 6.47) does not have a term to define the upper growth

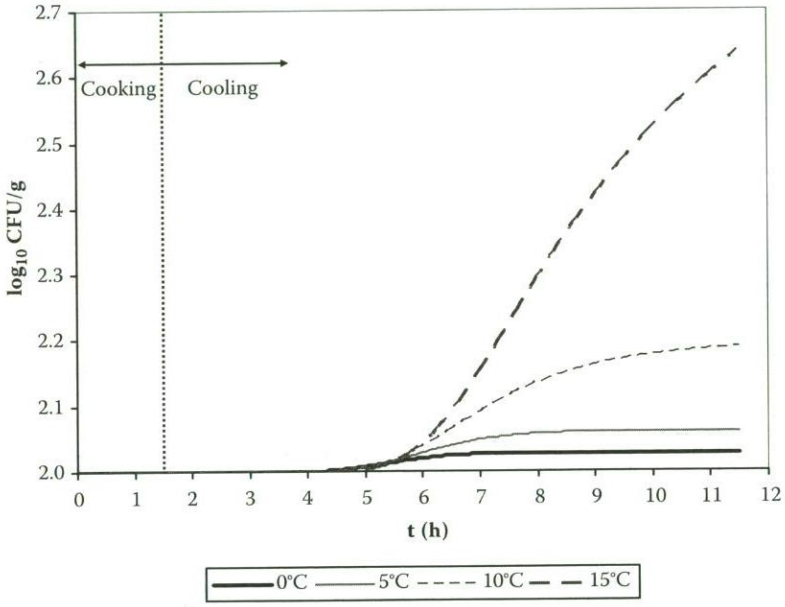

Figure 6.12 Estimation of growth of *C. perfringens* in cooked beef during cooling using the Huang 2004 approach. Shown in the figure is the estimated growth during a 10 h period with cooling air maintained at 0, 5, 10, and 15°C, respectively. The heat transfer coefficient during cooling was 10 W/m²s.

temperature limit, the growth rates estimated by this model were higher than those calculated by Eq. 6.45. Although an upper temperature was imposed during numerical analysis for the Baranyi model, the growth at temperatures above 42°C was overestimated, which led to slightly higher estimations than the Huang 2004 approach.

6.6.2.4 *Scenario 2—Effect of heat transfer coefficient on growth during cooling*

This example demonstrates the effect of reduced surface heat transfer coefficients during cooling on the growth of *C. perfringens* in cooked beef. The surface heat transfer coefficient measures the rate at which thermal energy is transferred from a solid surface to the ambient medium during cooling. A lower surface heat transfer coefficient suggests that the thermal energy is removed from cooked beef roasts in a less efficient manner. In the examples shown in the previous section, the surface heat transfer coefficient was set at 10 W/m²s. In this section, the surface heat transfer coefficient was set at 5 W/m²s during cooling.

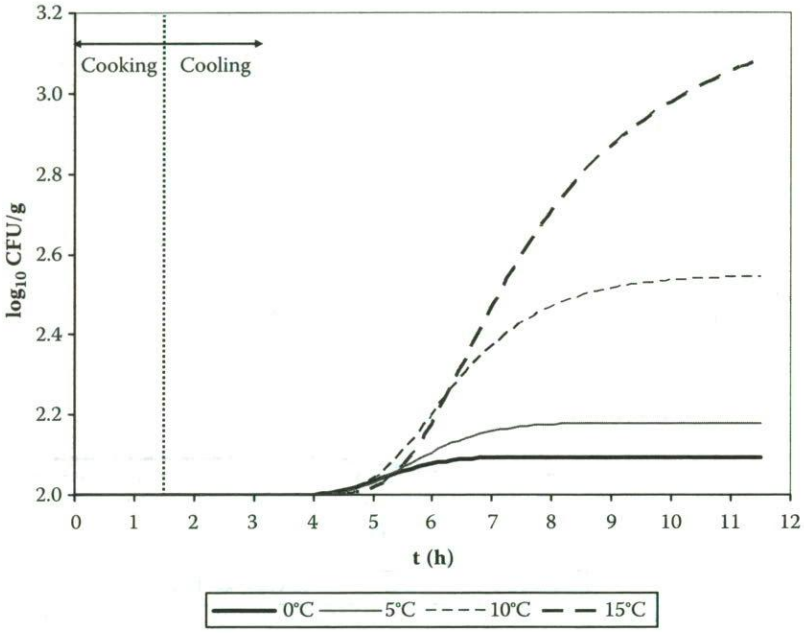

Figure 6.13 Estimation of growth of *C. perfringens* in cooked beef during cooling using the Baranyi model. Shown in the figure is the estimated growth during a 10 h period with cooling air maintained at 0, 5, 10, and 15°C, respectively. The heat transfer coefficient during cooling was 10 W/m²s.

With a reduced surface heat transfer coefficient, heat was removed at a much slower rate than the examples shown in the previous section. Figure 6.14 illustrates the effect of cooling temperature on the surface temperature of cooked beef roasts. It is apparent that the surface temperature is above the minimum growth temperature, except for the process with 0°C ambient temperature. At the geometric center, the time needed to pass through the temperature range of 51°C and 27°C was 3, 3.4, 4, and 5 h for cooling temperatures of 0, 5, 10, and 15°C, respectively, at the reduced heat transfer coefficient (Figure 6.15). The relative growth estimated by the Huang 2004 approach was 0.54, 0.97, 1.54, and 2.12 logs, as compared to 1.18, 1.71, 2.50, and 3.15 logs estimated by the Baranyi model. The relative growth estimated by the Baranyi model was slightly higher than the results estimated using the Huang 2004 approach. The difference in the estimation of relative growth is not caused by the primary model, but the difference in the secondary models.

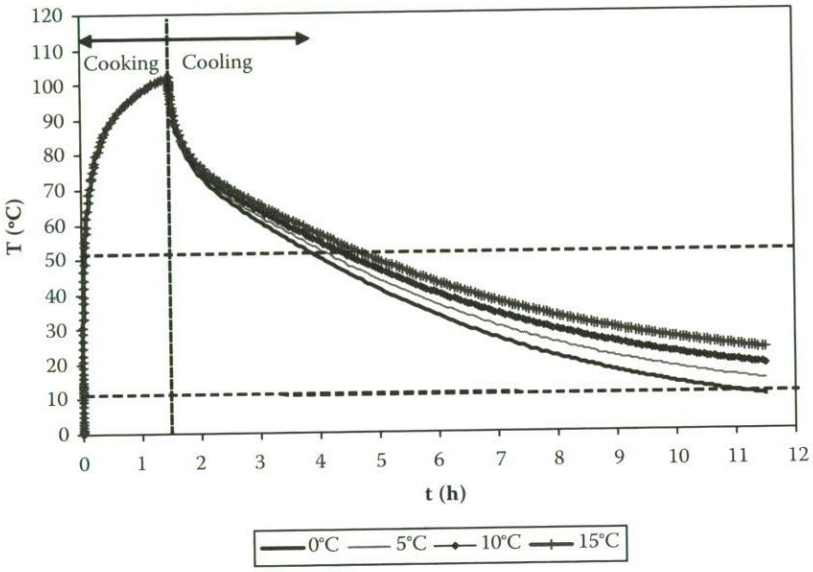

Figure 6.14 Simulated surface temperature histories during cooking and cooling of beef roasts. The legends represent cooling air temperatures. The dotted horizontal lines represent the upper and lower temperature limits. The heat transfer coefficient during cooling was 5 W/m^2s.

The computer simulation shown in these two sections clearly demonstrates the effects of cooling temperature and the surface heat transfer coefficient on the growth of *C. perfringens* during cooling. It also demonstrates that computer simulations can be used to estimate and evaluate the growth of *C. perfringens* in cooked meats during cooling in the event of process deviation.

6.7 Conclusions

In general, both empirical and mechanistic models can be used to describe the growth of *C. perfringens* in cooked meats under isothermal and dynamic conditions and achieve a reasonable degree of accuracy. Computer simulation can become a viable tool for evaluating the safety of cooked meat products exposed to temperature abuse at the stage of industrial production and commercial distribution. It suggested, however, that any model and computer simulation methodology be experimentally validated before being used in the real-world applications.

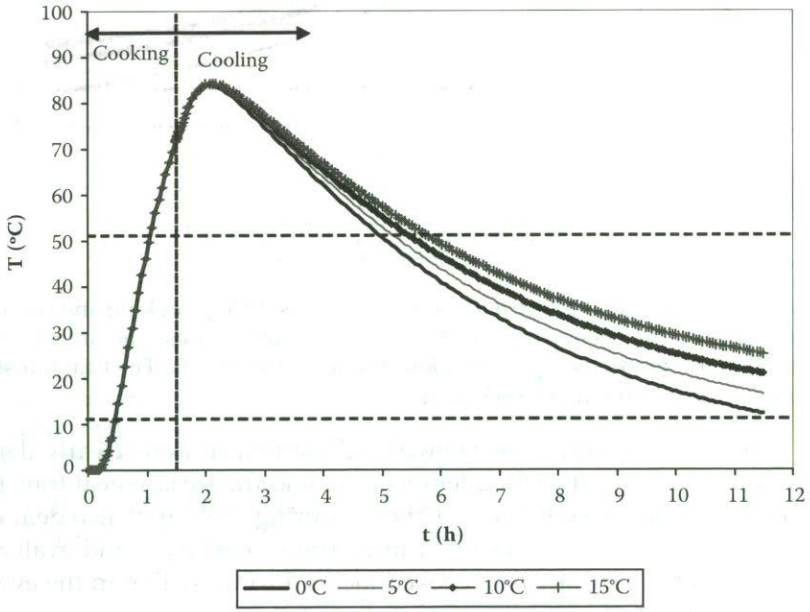

Figure 6.15 Simulated center temperature histories during cooking and cooling of beef roasts. The legends represent center temperatures. The dotted horizontal lines represent the upper and lower temperature limits. The heat transfer coefficient during cooling was 5 W/m²s.

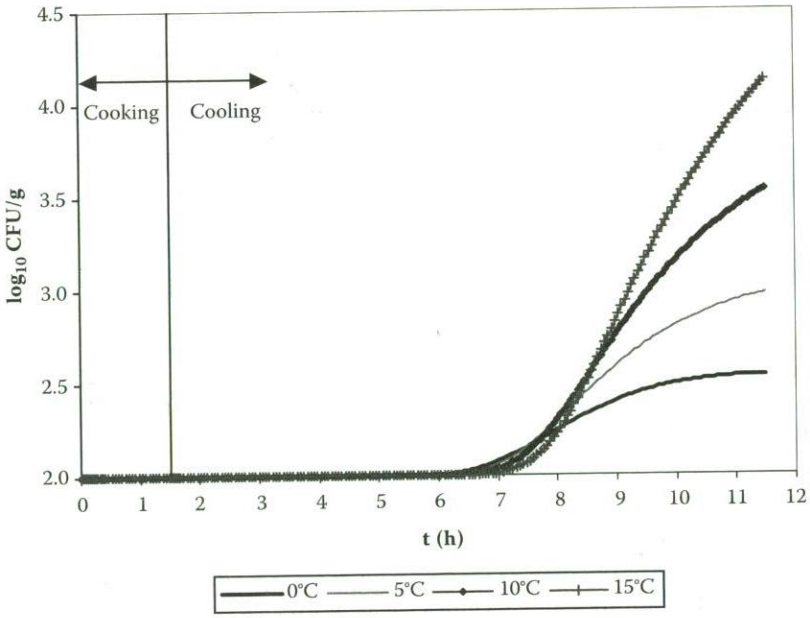

Figure 6.16 Estimation of growth of *C. perfringens* in cooked beef during cooling using the Huang 2004 approach. Shown in the figure is the estimated growth during a 10 h period with cooling air maintained at 0, 5, 10, and 15°C, respectively. The heat transfer coefficient during cooling was 5 W/m²s.

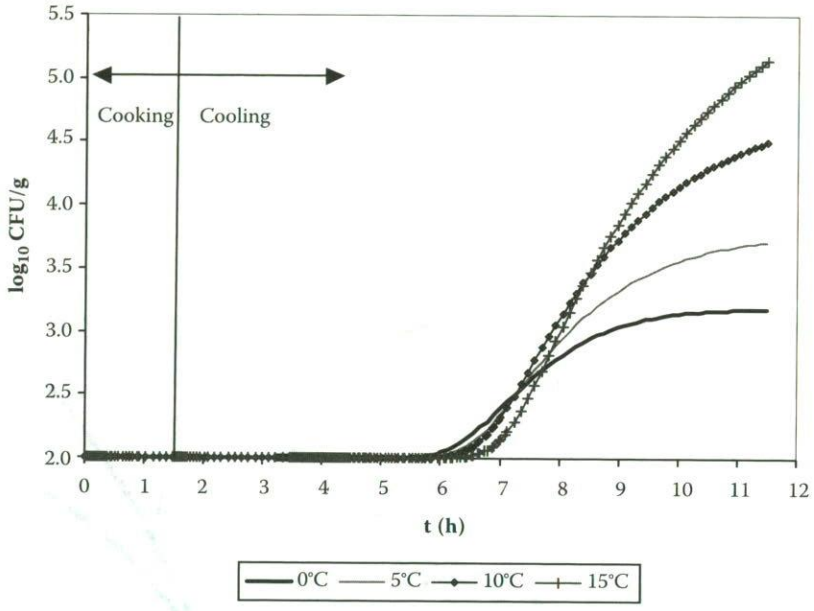

Figure 6.17 Estimation of growth of *C. perfringens* in cooked beef during cooling using the Baranyi model. Shown in the figure are the estimated growth during a 10 h period with cooling air maintained at 0, 5, 10, and 15°C, respectively. The heat transfer coefficient during cooling was 5 W/m²s.

References

Amezquita, A., Wang, L., and Weller, C. L. 2005. Finite element modeling and experimental validation of cooling rates of large ready-to-eat meat products in small meat-processing facilities. *Trans. ASAE.* 48(1):287–303.

Amezquita, A., Weller, C. L., Wang, L., Thippareddi, H., and Burton, D. E. 2005. Development of an integrated model for heat transfer and dynamic growth of *Clostridium perfringens* during the cooling of cooked boneless ham. *Int. J. Food Microbiol.* 101:123–44.

Baranyi, J., McClure, P. J., Sutherland, J. P., and Roberts, T. A. 1993. Modeling bacterial growth responses. *J. Ind. Microbiol.* 12:190–4.

Baranyi, J., and Roberts, T. A. 1994. A dynamic approach to predicting bacterial growth in food. *Int. J. Food Microbiol.* 23:277–94.

Baranyi, J., Roberts, T. A., and McClure, P. 1993. A non-autonomous differential equation to model bacterial growth. *Food Microbiol.* 10:43–59.

Baranyi, J., Robinson, T. P., Kaloti, A., and Mackey, B. M. 1995. Predicting growth of *Brochothrix thermosphacta* at changing temperature. *Int. J. Food Microbiol.* 27:61–75.

Brynestad, S., and Granum P. E. 2002. *Clostridium perfringens* and foodborne infections. *Int. J. Food Microbiol.* 74:195–202.

Chandra, P. K., and Singh, R. P. 1995. *Applied Numerical Methods for Food and Agricultural Engineers*. CRC Press, Boca Raton, FL.

Craven, D. E. 1980. Growth and sporulation of *Clostridium perfringens* in foods. *Food Tech.* 34(4):80–7, 95.

Hall, R. A., and Angelotti, R. 1965. *Clostridium perfringens* in meat and meat products. *Appl. Microbiol.* 13:352–6.

Huang, L. 2003. Dynamic computer simulation of *Clostridium perfringens* growth in cooked ground beef. *Int. J. Food Microbiol.* 87: 217–227.

Huang, L. 2004. Numerical analysis of the growth of *Clostridium perfringens* in cooked beef under isothermal and dynamic conditions. *J. Food Safety.* 24:53–70.

Huang, L. 2007. Numerical analysis of survival of *Listeria monocytogenes* during in-package pasteurization of frankfurters by hot water immersion. *J. Food Sci.* 72: E285–292.

Huang, L. 2008. Growth kinetics of *Listeria monocytogenes* in broth and beef frankfurters—determination of lag phase duration and exponential growth rate under isothermal conditions. *J. Food Sci.* 73:E235–42.

Incropera, F. P., and DeWitt, D. P. 1996. *Fundamentals of Heat and Mass Transfer.* 4th Edition. John Wiley & Sons, New York, NY.

Juneja, V. K., Huang, L., and Thippareddi, H. H. 2006. Predictive model for growth of *Clostridium perfringens* in cooked cured pork. *Int. J. Food Microbiol.* 110:85–92.

Juenja, V. K., and Marks, H. M. 1999. Proteolytic *Clostridium botulinum* growth at 12–48°C simulating the cooling of cooked meat: development of a predictive model. *Food Microbiol.* 16:583–92.

Juneja, V. K., and Marks, H. M. 2002. Predictive model for growth of *Clostridium perfringens* during cooling of cooked cured chicken. *Food Microbiol.* 19:313–27.

Juenja, V. K., Marmer, B. S., Phillips, J. G., and Palumbo, S. A. 1996. Interactive effects of temperature, initial pH, sodium chloride, and sodium pyrophosphate on the growth kinetics of *Clostridium perfringens*. *J. Food Prot.* 59:963–8.

Juneja, V. K., Novak, J. S., Marks, H. M., and Combas, D. E. 2001. Growth of *Clostridium perfringens* from spores inocula in cooked cured beef: development of a predictive model. *Inov. Food Sci. & Emerging Tech.* 2:289–301.

Juneja, V. K., Snyder, O. P., and Cygnarowicz-Provost, M. 1994. Influence of cooling rate on outgrowth of *Clostridium perfringens* spores in cooked ground beef. *J. Food Prot.* 57:1063–7.

Juneja, V. K., Whiting, R. C., Marks, H. M., and Snyder, O. P. 1999. Predictive model for growth of *Clostridium perfringens* at temperatures applicable to cooling of cooked meat. *Food Microbiol.* 15:335–49.

Obuz, E., Powell, T. H., and Dikeman, M. E. 2002. Simulation of cooking cylindrical beef roasts. *Leb. Wiss. Tech.* 35:637–44.

Rahman, S. 1996. *Food Properties Handbook*. CRC Press, Boca Raton, FL.

Ratkowsky, D. A., Lowry, R. K., McKeekin, T. A., Stokes, A. N., and Chandler, R. E. 1983. Model for bacterial culture growth rate through the entire biokinetic temperature range. *J. Bacteriol.* 154:1222–6.

Ratkowsky, D. A., Olley, J., McKeekin, T. A., and Ball, A. 1982. Relationship between temperature and growth rate of bacterial cultures. *J. Bacteriol.* 149:1–5.

Sheen, S., and Hayakawa, K. 1991. Finite difference simulation for heat conduction with phase change in an irregular food domain with volumetric change. *Int. J. Heat Mass Trans.* 34:1337–46.

Sheen, S., Tong, C. H., Fu, Y. C., and Lund, D. B. 1993. Lethality of thermal processes for food in anomalous-shaped plastic containers. *J. Food Eng.* 20:199–213.

Singh, R. P. 1992. Heating and cooling processes of foods. In *Handbook of Food Engineering*, ed. D. B. Lund and D. B. Heldman, 247–276. Marcel Dekker, New York, NY.

Willardsen, R. R., Busta, F. F., and Allen, C. E. 1979. Growth of *Clostridium perfringens* in three different beef media and fluid thioglycollate medium at static and constantly rising temperatures. *J. Food Prot.* 42:144–148.

Zwietering, M. H., De Koos, J. T., Hasenack, B. E., De Wit, J. C., and van't Riet, K. 1991. Modeling of bacterial growth as a function of temperature. *Appl. Environ. Microbiol.* 57:1094–101.